Inhibition of Prostate Cancer Bone Metastasis by Synthetic TF Antigen Mimic/Galectin-3 Inhibitor Lactulose-L-Leucine[1]

Olga V. Glinskii[*,†], Sudha Sud[‡], Valeri V. Mossine[§], Thomas P. Mawhinney[§], Douglas C. Anthony[¶,#], Gennadi V. Glinsky[**], Kenneth J. Pienta[‡,2] and Vladislav V. Glinsky[†,¶,2]

[*]Department of Medical Pharmacology and Physiology, University of Missouri, Columbia, MO, USA; [†]Harry S. Truman Memorial Veterans Hospital, Columbia, MO, USA; [‡]Departments of Internal Medicine and Urology, Michigan Center for Translational Pathology and the University of Michigan Comprehensive Cancer Center, Ann Arbor, MI, USA; [§]Department of Biochemistry, University of Missouri, Columbia, MO, USA; [¶]Department of Pathology and Anatomical Sciences, University of Missouri, Columbia, MO, USA; [#]Department of Neurology, University of Missouri, Columbia, MO, USA; [**]The Sanford-Burnham Medical Research Institute, La Jolla, CA, USA

Abstract

Currently incurable, prostate cancer metastasis has a remarkable ability to spread to the skeleton. Previous studies demonstrated that interactions mediated by the cancer-associated Thomsen-Friedenreich glycoantigen (TF-Ag) and the carbohydrate-binding protein galectin-3 play an important role in several rate-limiting steps of cancer metastasis such as metastatic cell adhesion to bone marrow endothelium, homotypic tumor cell aggregation, and clonogenic survival and growth. This study investigated the ability of a synthetic small-molecular-weight non-toxic carbohydrate-based TF-Ag mimic lactulose-L-leucine (Lac-L-Leu) to inhibit these processes in vitro and, ultimately, prostate cancer bone metastasis in vivo. Using an in vivo mouse model, based on intracardiac injection of human PC-3 prostate carcinoma cells stably expressing luciferase, we investigated the ability of Lac-L-Leu to impede the establishment and growth of bone metastasis. Parallel-flow chamber assay, homotypic aggregation assay, modified Boyden chamber assay, and clonogenic growth assay were used to assess the effects of Lac-L-Leu on tumor cell adhesion to the endothelium, homotypic tumor cell aggregation, transendothelial migration, and clonogenic survival and growth, respectively. We report that daily intraperitoneal administration of Lac-L-Leu resulted in a three-fold ($P < .05$) decrease in metastatic tumor burden compared with the untreated control. Mechanistically, the effect of Lac-L-Leu, which binds and inhibits galectins by mimicking essential structural features of the TF-Ag, was associated with a dose-dependent inhibition of prostate cancer cell adhesion to bone marrow

endothelium, homotypic aggregation, transendothelial migration, and clonogenic growth. We conclude that small-molecular-weight carbohydrate-based compounds targeting β-galactoside–mediated interactions could provide valuable means for controlling and preventing metastatic prostate cancer spread to the skeleton.

Neoplasia (2012) 14, 65–73

Introduction

Despite recent improvements in early detection and treatment, prostate cancer remains one of the most commonly diagnosed cancers worldwide and a second leading cause of cancer-related deaths among men in the United States [1,2]. The prevailing cause of morbidity and mortality associated with malignant neoplastic disease of the prostate is metastasis. Advanced prostate cancer almost inevitably metastasizes to the skeleton [3,4], bringing about devastating complications resulting in spinal cord compression, intractable pain, and, ultimately, death. At present, there is no effective means to control or prevent metastatic dissemination of hormone refractory prostate cancer.

Hematogenous spread of prostate cancer is an extremely complex process regulated on many levels and involving multiple rate-limiting steps [5–7]. Previous results from our group and those of others demonstrated that several critical steps in hematogenous cancer metastasis, including prostate cancer, are regulated in part by β-galactoside–mediated interactions involving cancer-associated Thomsen-Friedenreich carbohydrate antigen (TF-Ag) and β-galactoside–binding lectin galectin-3 (Gal-3). Specifically, Gal-3 was implicated in prostate cancer cell preferential adhesion to bone marrow endothelial cells [8]. TF-Ag/Gal-3 interactions were shown to mediate the adhesion of metastatic cells to the endothelium [9–16], homotypic cancer cell aggregation at the sites of primary attachment to the endothelium [13,17], the *in vivo* formation of intravascular metastatic deposits in lungs and bones of experimental animals after intravenous inoculation [12,16], as well as clonogenic survival and growth of metastatic cancer cell lines [17–19].

Importantly, all these processes representing critical rate-limiting steps in cancer metastasis could be inhibited efficiently using carbohydrate-based compounds blocking galectins by mimicking essential structural features of their natural ligands [9,19–22].

The concept of using carbohydrate-based galectin inhibitors for targeting cancer metastasis has been conceived by early pioneering works from the group of Dr Raz [23–25]. Subsequent discovery of Gal-3 functioning in various pathologic and physiological processes such as cell adhesion [26–29], angiogenesis [30,31], and regulation of apoptosis [32] attracted increasing attention of the research community, resulting in the development of carbohydrate-based galectin inhibitors by several different groups [33–39]. One such inhibitor, modified citrus pectin (MCP) developed by the group of Dr Raz [23–25], has been shown to inhibit experimental metastasis *in vivo* in several animal models, notably mouse B16 melanoma [23,24], rat MAT-LyLu prostate carcinoma [25], human MDA-MB-435 breast carcinoma [20], and human LSLiM6 colon carcinoma [20].

Another carbohydrate-based galectin inhibitor developed by this group, the synthetic β-galactoside disaccharide/amino acid conjugate, glycoamine lactulose-L-leucine (Lac-L-Leu), binds and inhibits Gal-3 by mimicking cancer-associated TF-Ag [9,10,17]. This compound's TF-Ag–mimicking properties were confirmed through inhibition of TF-Ag/polyacrylamide conjugate binding to cancer cells, blocking binding of TF-Ag–specific PNA lectin to asialofetuin, and inhibiting Gal-3 interactions with TF-Ag conjugated to human serum albumin [9]. Consequently, Lac-L-Leu has been shown to impede *in vitro* and *ex vivo* heterotypic (between tumor and endothelial cells) and homotypic (between tumor cells) metastasis-associated tumor cell adhesive interactions including DU-145 human prostate cancer cells [9,10,12–17], the *in vivo* formation of early metastatic deposits in lungs and bones by human breast (MDA-MB-435) and prostate (DU-145) cells [12,16], the *in vitro* clonogenic survival and growth of several different types of cancer [17–19], and ultimately MDA-MB-435 and MDA-MB-435Lung2 human breast carcinoma spontaneous lung metastasis in nude mice [19,22]. To date, however, carbohydrate-based galectin inhibitors have not been tested yet *in vivo* against human prostate cancer bone metastasis.

In this study, we used the *in vivo* bone metastasis model based on the intracardiac injection of PC-3Luc cells [40] to investigate the ability of Lac-L-Leu to affect the establishment and development of prostate cancer metastatic bone lesions. We report that daily treatment of experimental animals with nontoxic carbohydrate-based small-molecular-weight galectin inhibitor Lac-L-Leu without any addition of cytotoxic drugs resulted in a three-fold inhibition of prostate cancer bone metastasis. Mechanistically, the Lac-L-Leu effects were associated with the inhibition of prostate cancer cell adhesion to bone marrow endothelium, their homotypic aggregation, transendothelial migration, as well as clonogenic survival and growth, suggesting that this compound affects both the establishment and the early development of prostate cancer bone metastasis.

Materials and Methods

Chemicals and Reagents

Synthetic glycoamines lactulose-L-leucine (Lac-L-Leu; *N*-(1-deoxy-4-*O*-(β-D-galactopyranos-1-yl)-D-fructos-1-yl)-(*S*)-2-amino-4-methyl-pentanoic acid) and lactitol-L-leucine (Lct-L-Leu; *N*-(1-deoxy-4-*O*-(β-D-galactopyranos-1-yl)-D-glucitol-1-yl)-(*S*)-2-amino-4-methylpentanoic acid) were synthesized as previously described [21]. All other chemicals and reagents, unless otherwise specified, were purchased from Sigma (St Louis, MO).

Cell Lines and Cultures

PC-3Luc cell line was developed previously using stable transfection of metastatic human prostate carcinoma PC-3 (ATCC, Rockville, MD) with luciferase-expressing pLazarus retroviral vector [40]. The DU-145 human prostate carcinoma cells were purchased from ATCC. Tumor cell lines were routinely maintained on plastic as monolayer cultures using RPMI-1640 medium supplemented with 10% fetal bovine serum (FBS) in a 5% CO_2 humidified incubator. The development of human bone marrow endothelial cell line HBME-1, which was used in parallel-flow chamber experiments, was described previously

[8]. HBME-1 cells were cultured in Dulbecco modified Eagle medium supplemented with L-glutamine, 10% FBS, and sodium pyruvate.

In Vivo *Bioluminescent Model of Metastatic Prostate Cancer Growth*

Animal experiments were conducted according to the University of Michigan's Institutional Animal Care and Use Committee approved protocol. Briefly, 5- to 6-week-old male severe combined immuno-deficient mice ($n = 30$) purchased from Charles River (Wilmington, MA) were randomly divided into three groups ($n = 10$ animals per group). In all three groups, PC-3Luc cells (2×10^5 cells in 100 µl of Dulbecco phosphate-buffered saline [PBS] lacking Ca^{2+} and Mg^{2+}) were introduced into animals by intracardiac injection under 1.75% isoflurane/air anesthesia. Throughout the duration of the experiment, animals in group 1 were receiving daily 20 µM of Lac-L-Leu administered intraperitoneally (i.p.) in 0.2 ml of sterile physiological saline beginning 1 week before tumor cell inoculation. In group 2, animals were receiving 20 µM of Lac-L-Leu daily administered i.p. in 0.2 ml of sterile physiological saline beginning 1 week after tumor cell inoculation. In group 3 (untreated control), animals were receiving daily 0.2 ml i.p. injection of the vehicle, sterile physiological saline. Bioluminescent imaging of PC-3Luc was performed as previously described [40,41] through the University of Michigan Small Animal Imaging Resource facility. Mice were serially imaged weekly for 5 weeks using a CCD IVIS system with a 50-mm lens (Xenogen Corp, Alameda, CA), and the results were analyzed using Living Image software (Xenogen). For imaging, mice were injected with luciferin (40 mg/ml) i.p., and ventral images were acquired 15 minutes after injection under 1.75% isoflurane/air anesthesia. For each animal, total tumor burden was calculated using regions of interest. At the end of the experiments, animals were killed, and tissue was collected for histopathologic confirmation of bone metastasis.

In Vitro *Parallel-Flow Chamber Assay*

The adhesion of PC-3Luc and DU-145 cells to the monolayers of human bone marrow endothelial cells was studied in an *in vitro* parallel-plate laminar flow chamber as follows. HBME-1 cells were grown until 100% confluent in 35-mm tissue culture dishes coated overnight with poly-L-lysine (10 µg/ml) at 4°C. The parallel-plate flow chamber deck with a 100-µm gasket (Glycotech, Rockville, MD) was assembled over the endothelial monolayer, and endothelial cells were exposed to flow conditions (0.8 dyn/cm² shear stress) by perfusing warm medium (RPMI-1640 containing 0.75 mM Ca^{2+} and Mg^{2+} and 0.2% human serum albumin) using a constant infusion/withdrawal syringe pump (KDS210; KD Scientific, New Hope, PA). Next, a single-cell suspension of cancer cells (5×10^4 cells/ml) was perfused for a 15-minute period in the presence or absence of 200 µM of synthetic glycoamines (Lac-L-Leu or Lct-L-Leu). Tumor cell interactions with HBME-1 monolayers were observed by using an inverted phase-contrast Diavert microscope (Leitz, Wetzlar, Germany) and video recorded in three different observation fields (5 minutes per field) for subsequent frame-by-frame analysis. The number of rolling cells and the number of stably adherent cells per field were determined during 1- and 5-minute periods, respectively, in at least three different observation fields for each experimental setting. Data are presented as means ± SD.

Homotypic Aggregation Assay

The effect of various concentrations (0-1.0 mM) of the Lac-L-Leu and Lct-L-Leu on PC-3Luc prostate carcinoma cell spontaneous aggregation was assessed using a homotypic aggregation assay as previously

described [13,22]. Briefly, cells were detached from the tissue culture plates with PBS containing 2 mM EDTA, washed with PBS, and re-suspended to a density of 1×10^6 cells/ml in serum-free RPMI 1640 media. Next, tumor cell suspension (500 µl containing 5×10^5 cells) was mixed with 500 µl of serum-free medium in the presence of increasing concentrations (0-1.0 mM final concentration) of the Lac-L-Leu or the control glycoamine Lct-L-Leu. Plastic tubes containing cancer cells were placed in a rotator and agitated for 1 hour at 37°C. After the incubation, three 25-µl aliquots from each sample were spotted onto a microscope slide and dried for 1 hour at room temperature. The slides were fixed overnight in a closed container with 37% form-aldehyde in a bottom reservoir. Immediately before microscopic evaluation, 25 µl of PBS was placed onto each spot to facilitate viewing. The total number of cells and the number of cells in aggregates were counted in four random fields. The percent of cells in aggregates (number of cells in aggregates / total number of cells × 100) and the average number of aggregated cells were calculated for individual samples. Each assay was performed in triplicate. Results are presented as means ± SD.

Transendothelial Migration

Endothelial cells (2×10^4) were seeded into the 24-well collagen type I–coated Biocoat cell culture inserts (Becton Dickinson, Bedford, MA) with 3-µm-pore-size track-etched PET membranes permitting cell viewing by light microscopy and were grown for 5 days until fully confluent. Next, 1×10^4 of GFP-tagged PC-3 or DU-145 cells were added to each well in 5% FBS medium with or without compound tested and allowed to interact overnight while using 20% FBS medium in the lower chamber as a chemoattractant. The next day, the cells in the upper chamber were gently wiped with cotton swab, and the transmi-grated cells were photographed on a lower surface of the membrane using an epifluorescent microscope. Images of four fields (1 field for each quadrant of the membrane) were acquired using a 10× lens. The assays were performed in quadruplicate for each experimental setting, and results are presented as means ± SD.

Clonogenic Survival and Growth

The PC-3Luc or DU-145 cells, grown until 50% to 60% confluent, were harvested using a nonenzymatic cell dissociation reagent as described above and plated at a low density in quadruplicate (100 and 200 viable cells per well) in a 24-well culture plate without (control) or in the presence of compounds tested. Only cells with a viability of 95% or greater were used. Seven days later, the cells were fixed with 1% formaldehyde in PBS and stained with hematoxylin, and colonies of more than 15 cells were scored.

Statistical Analysis

The 2-tailed paired Student's *t* test or one-way analysis of variance (for multiple group comparison) was used to assess statistical significance of the results. χ^2 analysis was used to compare metastatic tumor burden distribution between the groups. The difference between the groups was considered significant at $P \leq .05$.

Results and Discussion

Lac-L-Leu Inhibits PC-3Luc Bone Metastasis In Vivo

Prostate cancer bone metastasis model based on intracardiac injection of PC-3Luc cells is perhaps the only currently available model recapitulating both hematogenous steps involved in prostate cancer metastatic spread and many of the clinical features of prostate cancer

metastasis [40]. Owing to a constitutive expression of firefly luciferase in PC-3Luc cells, this experimental system allows for a nondestructive quantitative imaging of metastatic lesions (Figure 1A) to monitor temporal dynamics of disease progression and effects of therapeutic interventions in individual animals (Figure 2A). A detailed postmortem histopathologic examination performed at the end of the experiment confirms the presence of metastatic tumor cells in the skeletal lesions (Figure 1, B-D). Of note, although metastatic tumor burden in this model is mostly associated with bone colonization, soft tissue (adrenal gland, liver, lung, and lymph node) metastases could be observed as well [40]. However, because the focus of this study was on bone metastasis, we only confirmed histopathologically metastatic lesions detected by bioluminescent imaging in femoral, tibial, mandibular, and nasal bones of experimental animals and did not perform soft tissue histology.

In the current study, we used this experimental system to investigate effects of the TF-Ag mimic, synthetic carbohydrate-based Gal-3 inhibitor Lac-L-Leu, on the establishment and growth of PC-3Luc bone metastasis. In these experiments, the animals were divided into three groups receiving systemic treatment as follows: Lac-L-Leu beginning 1 week before tumor cell inoculation (group 1), Lac-L-Leu beginning 1 week after tumor cell inoculation (group 2), vehicle (sterile physiological saline) only (group 3/control). In all three groups, the animals were imaged weekly throughout the duration of the study (up to 4 weeks after tumor cell injection) beginning from the day of tumor cell inoculation.

The results of these experiments (Figure 2) demonstrated the strongest beneficial effect for Lac-L-Leu administered to the mice beginning 1 week before PC-3Luc cell inoculation (group 1), compared with the postinoculation treatment (group 2) or the untreated control (group 3). On the basis of the photon counts, temporal dynamics of metastatic tumor burden in individual animals between the groups has been clearly separated as follows: group 1 < group 2 < control (Figure 2A). At week 4 after tumor cell injection, metastatic tumor burden in group 1 animals was approximately three-fold ($P < .05$) less than in control (Figure 2B). In group 2, however, because three animals were lost early in the experiment to unknown causes, the number of mice was reduced to $n = 7$. Consequently, the difference between average photon counts in group 2 and control did not reach statistical significance because of insufficient power (Figure 2B). However, χ^2 analysis of metastatic tumor burden distribution within the groups demonstrates that both groups 1 and 2 indeed differed significantly from the control (Table 1).

Furthermore, groups 1 and 2 also differ significantly from each other ($P = .05$, t-test; $P = .0168$, χ^2 test). The more pronounced protective effect of Lac-L-Leu against PC-3Luc bone metastasis in group 1 (in which treatment commenced 1 week before tumor cell injection) compared with group 2 (in which treatment commenced 1 week after tumor cell inoculation) and untreated control indicates that the compound inhibits both the process of metastatic lesion establishment and the growth of early metastatic colonies. Thus, we investigated next how Lac-L-Leu affects prostate cancer cell metastasis–associated heterotypic (with bone marrow endothelial cells) and homotypic (with each other) adhesive interactions, their transendothelial migration, as well as clonogenic survival and growth.
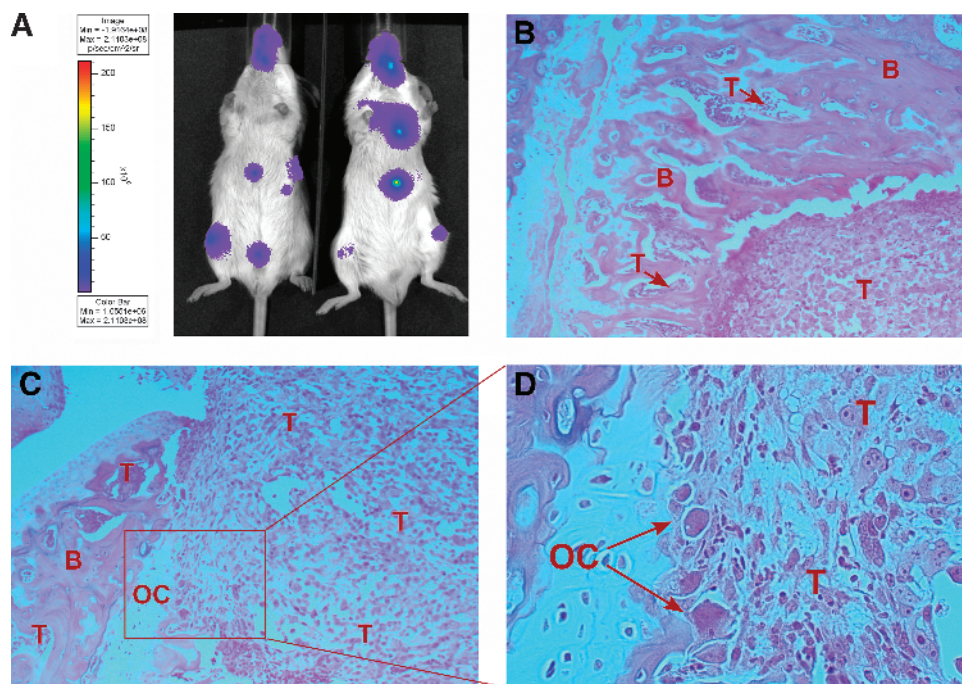

Figure 1. Intravital bioluminescent imaging of PC-3Luc metastatic burden and subsequent postmortem histopathologic confirmation of skeletal metastases. (A) An example of the bioluminescent imaging using a CCD IVIS system showing PC-3Luc metastatic tumors to the limbs, jaws, and ribs. Two animals from the control group are shown at week 3 after tumor cell injection. A color scale reflecting photon count in pseudocolored images is shown on the left. (B-D) Histopathologic confirmation and analysis of skeletal metastases. (B) Photomicrograph of PC-3Luc bone metastasis (hematoxylin and eosin, decalcified; original magnification, ×10). A tumor mass (T) is present in the marrow cavity, as well as smaller tumor cell clusters (T + arrow) in the cortical bone (B). (C and D) Osteoclast-like cells (OC), commonly associated with bone metastases, are present at the interface between the tumor (T) and the cortical bone (B) (hematoxylin and eosin, decalcified; original magnification, ×10 [C] and ×40 [D]).
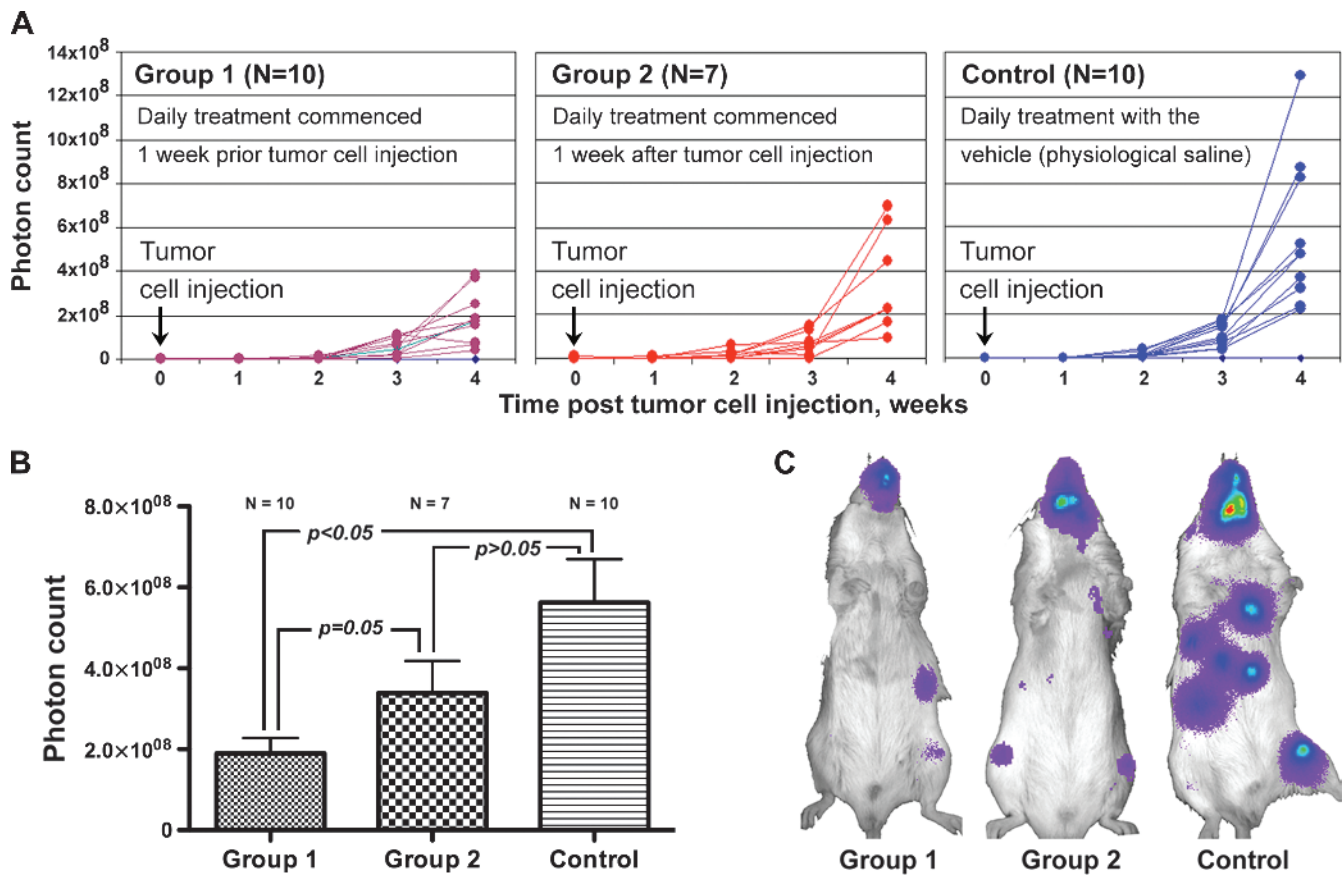
Figure 2. The effect of Lac-L-Leu treatment on PC-3Luc bone metastasis. (A) Temporal dynamics of changes in metastatic tumor burden in individual animals from group 1 (daily Lac-L-Leu treatment commenced 1 week before tumor cell injection), group 2 (daily Lac-L-Leu treatment commenced 1 week after tumor cell injection), and control during the 4 weeks after intracardiac tumor cell inoculation as revealed by biophoton count. (B) Cumulative data showing average metastatic tumor burden in each experimental group at week 4 after tumor cell inoculation. Data are presented as means ± SEM. (C) Representative images of animals from each experimental group at 4 weeks after tumor cell injection.

Lac-L-Leu Inhibits PC-3Luc and DU-145 Metastasis-Associated Adhesive Interactions

Previous studies demonstrated that TF-Ag/Gal-3–mediated interactions support both metastatic cell adhesion to the endothelium and their homotypic aggregation at the sites of primary attachment to the vascular wall [9–17]. Therefore, we have used a parallel-flow chamber assay to investigate the effect of TF-Ag mimic Lac-L-Leu on PC-3Luc and DU-145 adhesive interactions with monolayers of HBME-1 human bone marrow endothelial cells under conditions of physiological (0.8 dyn/cm^2) wall shear stress. Another synthetic glycoamine Lct-L-Leu, which is an inactive isomer of Lac-L-Leu [9], was used as a negative control in these experiments. The results of the parallel-flow chamber

experiments (Figure 3A) demonstrated that Lac-L-Leu inhibited PC-3Luc and DU-145 cell rolling on HBME-1 monolayers 3.5- to 4.5-fold ($P < .05$) and stable adhesion 11.5-fold ($P < .01$), respectively. In contrast, Lct-L-Leu failed to inhibit prostate cancer cell adhesive interactions with endothelial cells. Similarly, Lac-L-Leu (but not Lct-L-Leu) inhibited PC-3Luc and DU-145 homotypic aggregate formation in a dose-dependent manner (Figure 3, B and C). These results indicate that Lac-L-Leu efficiently inhibits intravascular metastasis–associated prostate cancer cell adhesive interactions. In addition, the fact that Lac-L-Leu, but not Lct-L-Leu, exhibits inhibitory activity toward PC-3Luc metastasis–associated interactions indicates that this property of the compound depends entirely on its carbohydrate moiety and aptitude to mimic TF-Ag. The only difference between lactulose and lactitol is that glucose in the latter disaccharide is in the open (alcohol) form. However, this modification abolishes inhibitory properties of the compound owing to a nearly complete lack of lactitol affinity to Gal-3 [42].

Lac-L-Leu Inhibits PC-3Luc and DU-145 Transendothelial Migration and Clonogenic Growth

Next, we investigated whether blocking TF-Ag/Gal-3–mediated interactions with Lac-L-Leu affects subsequent steps of the metastatic

Table 1. χ^2 Analysis of Metastatic Tumor Burden Distribution within Experimental Groups Based on Biophoton Count.

	Threshold 1 (2×10^8 Photon per Second)		Threshold 2 (3×10^8 Photon per Second)	
	Percent above Threshold	$P (\chi^2)$	Percent above Threshold	$P (\chi^2)$
Group 1	30% (3/10)	<.0001	20% (2/10)	<.0001
Group 2	71% (5/7)	.0433	43% (3/7)	.014
Control	100% (10/10)		80% (8/10)	

cascade such as tumor cell transendothelial migration and their clonogenic survival and growth. We have used transwell migration assay to assess the effect of Lac-L-Leu and Lct-L-Leu on the ability of prostate cancer cells to traverse endothelial monolayers. The results of these experiments (Figure 4, *A* and *B*) demonstrated that Lac-L-Leu, but not Lct-L-Leu, efficiently inhibited PC-3 and DU-145 cell migration through the monolayers of endothelial cells ($P < .01$). The compound also inhibited clonogenic survival and growth of PC-3Luc and DU-145 cells in a dose-dependent manner (Figure 4*C*).

In summary, our *in vitro* experiments show that synthetic TF-Ag mimic Lac-L-Leu is inhibiting prostate cancer cell adhesive interactions with endothelial cells (rolling and stable adhesion), the formation of tumor cell multicellular aggregates (homotypic aggregation), transendothelial migration, and clonogenic survival and growth, indicating that TF-Ag–mediated interactions are involved in multiple aspects of prostate cancer metastasis to the skeleton. *In vivo*, these effects translate onto intravascular metastasis-associated events (initial metastatic cell arrest in distant organ microvasculature), tumor cell

extravasation, and survival and growth of early metastatic colonies. This explains the difference in the therapeutic effects achieved by Lac-L-Leu in two treatment groups. That is, the more pronounced effect in group 1 (daily Lac-L-Leu therapy commenced 1 week before tumor cell injection) was associated with the inhibitory effects on both the establishment and the development of early metastatic colonies, whereas in group 2 (daily Lac-L-Leu therapy commenced 1 week after tumor cell injection), only the effect on survival and clonogenic growth of micrometastases was present.

For a proper understanding of the mechanisms of action of Lac-L-Leu, it is important to recognize that the compound targets Gal-3 in different cell types and locations to inhibit different metastasis-associated processes (Figure 5). Previously, we demonstrated that TF-Ag induces Gal-3 translocation to the outer cell membranes in both endothelial and cancer cells [9,15,17] and then uses it as a binding partner to mediate heterotypic and homotypic adhesion respectively [9,15,17]. Thus, heterotypic adhesive interactions between tumor and endothelial cells (Figure 5*A*) are inhibited by Lac-L-Leu through blocking Gal-3
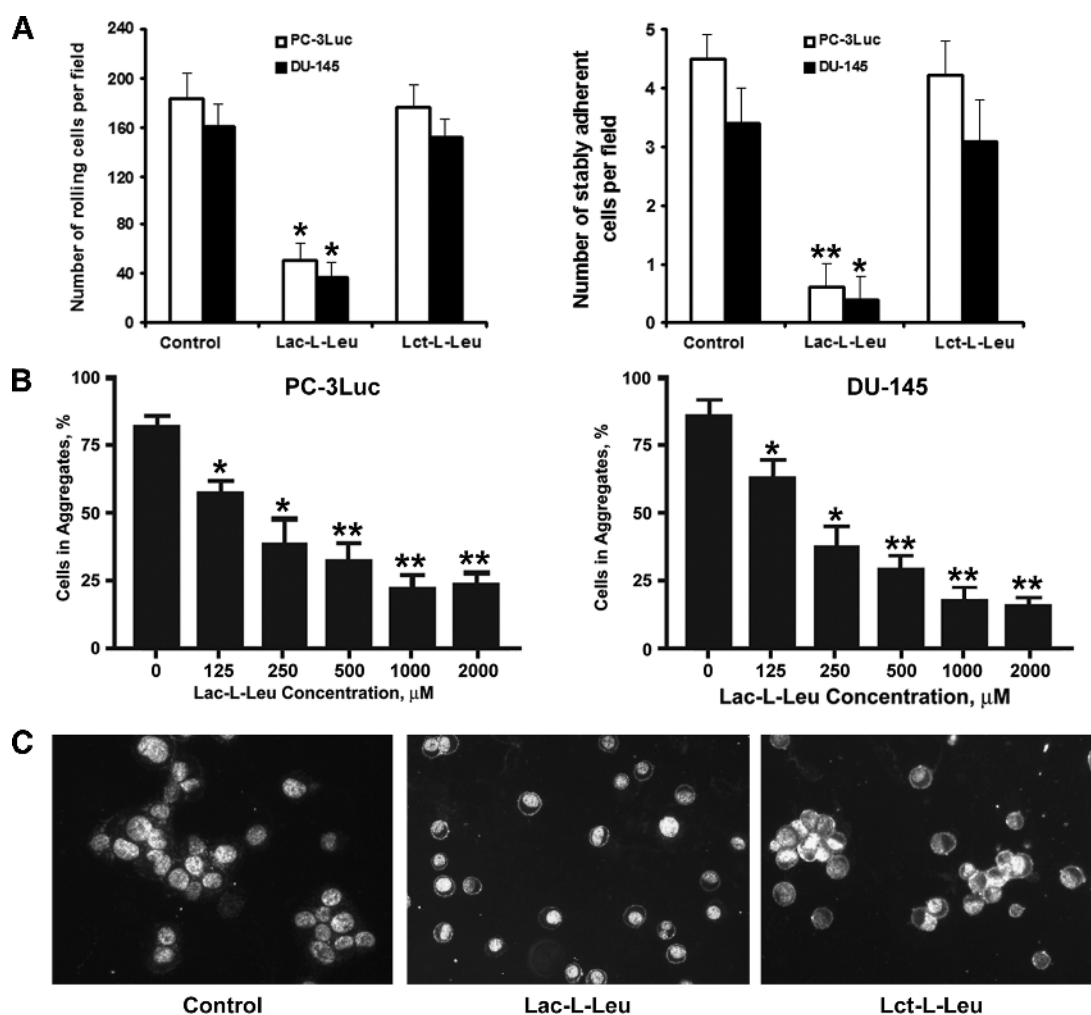

Figure 3. Inhibition of PC-3Luc and DU-145 metastasis-associated adhesive interactions by Lac-L-Leu. (A) Synthetic TF-Ag mimic Lac-L-Leu, but not Lct-L-Leu, inhibited PC-3Luc (open bars) and DU-145 (closed bars) rolling on (left panel) and stable adhesion (right panel) to HBME-1 human bone barrow endothelial cell monolayers under conditions of physiological flow. (B and C) Synthetic TF-Ag mimic Lac-L-Leu inhibited PC-3Luc (left panel) and DU-145 (right panel) tumor cell homotypic aggregation in a dose-dependent manner (B), whereas its inactive isomer Lct-L-Leu failed to inhibit the formation of prostate cancer cell multicellular aggregates (C). The experiments in A and C were performed using 200 μM (final concentration) of the compounds tested. *$P < .05$, **$P < .001$.
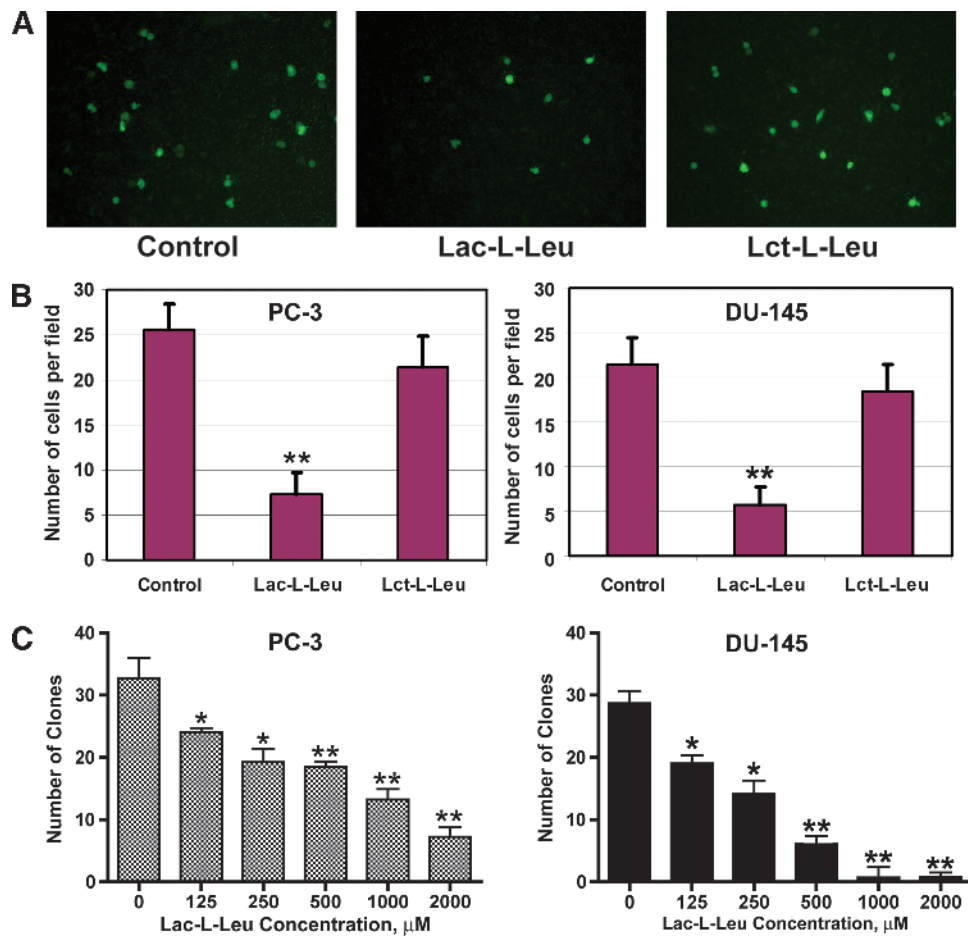
Figure 4. Inhibition of prostate cancer cell transendothelial migration and clonogenic growth by synthetic TF-Ag mimic Lac-L-Leu. (A and B) Synthetic TF-Ag mimic Lac-L-Leu, but not its inactive isomer Lct-L-Leu, inhibited PC-3 and DU-145 cell transendothelial migration *in vitro* in transwell chamber experiments. (C) Dose-dependent inhibition of PC-3Luc (left panel) and DU-145 (right panel) cell clonogenic survival and growth by synthetic glycoamine Lac-L-Leu. $*P < .05$, $**P < .001$.

translocated to the endothelial cell surfaces in response to TF-Ag [9,15,17]. Consequently, this inhibitory effect of Lac-L-Leu does not depend on the expression of Gal-3 in tumor cells. To inhibit the formation of homotypic tumor cell aggregates (Figure 5*B*), Lac-L-Leu binds and blocks Gal-3 clustered on the outer cell membranes of cancer cells [10,17]. Thus, the inhibitory effects of Lac-L-Leu on heterotypic and homotypic metastatic cell adhesive interactions occur through a direct competitive blockage of TF-Ag interactions with Gal-3 localized to the endothelial (Figure 5*A*) and tumor (Figure 5*B*) cell surfaces, respectively. In contrast, the effect of the compound on metastatic cell clonogenic survival and growth is due at least in part to the inhibition of intracellular Gal-3 antiapoptotic function on mitochondrial apoptosis pathway (Figure 5*C*). In our previous studies, we demonstrated that, in a process of clonogenic survival, most metastatic tumor cells die from
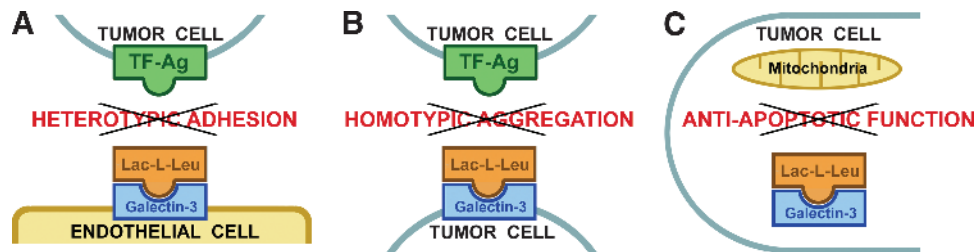

Figure 5. Lac-L-Leu mechanisms of action. (A) Heterotypic adhesive interactions between endothelial and cancer cells are inhibited through Lac-L-Leu binding to Gal-3 on endothelial cell surfaces preventing its interactions with TF-Ag presented on tumor cells. (B) Inhibition of tumor cell homotypic aggregation is achieved by blocking Gal-3 clustered on cancer cell outer membranes. (C) Inhibition of intracellular Gal-3 antiapoptotic function on mitochondrial apoptosis pathway reduces metastatic cell clonogenic survival.

apoptosis [18,19], executed through intrinsic, mitochondrial pathway [19], and Lac-L-Leu enhances tumor cell apoptotic death by inhibiting Gal-3 antiapoptotic function [19]. Among carbohydrate-based galectin inhibitors, the ability to block Gal-3 antiapoptotic function and suppress tumor cell clonogenic survival is not unique to Lac-L-Leu. MCP also efficiently inhibits tumor cell clonogenic survival by blocking Gal-3 antiapoptotic function [18]. Thus, both antiadhesive properties of carbohydrate-based galectin inhibitors and their ability to inhibit Gal-3 antiapoptotic function could be used to target the establishment and development of metastatic lesions. Moreover, because of the important role played by Gal-3 in regulating tumor cell apoptosis (reviewed in Nakahara et al. [32]), the ability of carbohydrate-based galectin inhibitors to impede Gal-3 antiapoptotic function on the mitochondrial pathway could be exploited further to increase the efficacy of cytotoxic therapies [18,19,32,43,44]. Indeed, inhibition of Gal-3 antiapoptotic function by MCP (also known as GCS-100) was sufficient to reverse multiple myeloma cell resistance to bortezomib and enhance their response to apoptosis induced by dexamethasone [45], cause 10.7-fold reduction of doxorubicin IC_{50} *in vitro* against hemangiosarcoma cells [18], and increase PC-3 cell sensitivity to cisplatin-induced apoptosis [46]. Similarly, blocking Gal-3 antiapoptotic function using Lac-L-Leu resulted in a 7.0-fold decrease in taxol IC_{50} *in vitro* against breast carcinoma cells [19] and in a 3.6-fold decrease in doxorubicin IC_{50} *in vitro* against hemangiosarcoma cells [18] and caused eradication of advanced metastatic disease *in vivo* in 56% of experimental animals with established breast cancer metastases treated with the Lac-L-Leu/paclitaxel combination [19]. Thus, it seems that the most promising clinical use of this class of compounds would be not only as single agents to block metastasis-associated adhesive events but also in combination with cytotoxic drugs to augment their effect on metastatic disease. Furthermore, such combination therapy regimens could be tailored to target metastatic cells when they still reside within intravascular compartment [47] as well as against circulating tumor cells.

In conclusion, it is quite remarkable that a simple nontoxic carbohydrate-based compound is capable of inhibiting three-fold metastatic burden associated with prostate cancer spread to the skeleton without addition of any cytotoxic drugs. In addition to Lac-L-Leu, other carbohydrate-based galectin inhibitors have been reported in the literature by different groups [33–39]. The results presented in this study suggest that this class of compounds holds strong potential of being developed into a valuable addition to the armamentarium of antimetastatic agents for controlling prostate cancer spread to the skeleton.

References

[1] Siegel R, Ward E, Brawley O, and Jemal A (2011). Cancer statistics, 2011: the impact of eliminating socioeconomic and racial disparities on premature cancer deaths. *CA Cancer J Clin* **61**, 212–236.

[2] Jemal A, Bray F, Center MM, Ferlay J, Ward E, and Forman D (2011). Global cancer statistics. *CA Cancer J Clin* **61**, 69–90.

[3] Mehra R, Kumar-Sinha C, Shankar S, Lonigro RJ, Jing X, Philips NE, Siddiqui J, Siddiqui J, Han B, Cao X, et al. (2011). Characterization of bone metastases from rapid autopsies of prostate cancer patients. *Clin Cancer Res* **17**, 3924–3932.

[4] Rubens RD (1998). Bone metastases—the clinical problem. *Eur J Cancer* **34**, 210–213.

[5] Roodman GD (2004). Mechanisms of bone metastasis. *N Engl J Med* **350**, 1655–1664.

[6] Tantivejkul K, Kalikin LM, and Pienta KJ (2004). Dynamic process of prostate cancer metastasis to bone. *J Cell Biochem* **91**, 706–717.

[7] Glinsky VV (2006). Intravascular cell-to-cell adhesive interactions and bone metastasis. *Cancer Metastasis Rev* **25**, 531–540.

[8] Lehr JE and Pienta KJ (1998). Preferential adhesion of prostate cancer cells to a human bone marrow endothelial cell line. *J Natl Cancer Inst* **90**, 118–123.

[9] Glinsky VV, Glinsky GV, Rittenhouse-Olsen K, Huflejt ME, Glinskii OV, Deutscher SL, and Quinn TP (2001). The role of Thomsen-Friedenreich antigen in adhesion of human breast and prostate cancer cells to the endothelium. *Cancer Res* **61**, 4851–4857.

[10] Khaldoyanidi SK, Glinsky VV, Sikora L, Glinskii AB, Mossine VV, Quinn TP, Glinsky GV, and Sriramarao P (2003). MDA-MB-435 human breast carcinoma cell homo- and heterotypic adhesion under flow conditions is mediated in part by Thomsen-Friedenreich antigen–galectin-3 interactions. *J Biol Chem* **278**, 4127–4134.

[11] Shekhar MP, Nangia-Makker P, Tait L, Miller F, and Raz A (2004). Alterations in galectin-3 expression and distribution correlate with breast cancer progression: functional analysis of galectin-3 in breast epithelial-endothelial interactions. *Am J Pathol* **165**, 1931–1941.

[12] Heimburg J, Yan J, Morey S, Wild L, Glinskii OV, Huxley VH, Klick R, Roy R, Glinsky VV, and Rittenhouse-Olson K (2006). Inhibition of spontaneous breast cancer metastasis by anti–Thomsen-Friedenreich antigen monoclonal antibody JAA-F11. *Neoplasia* **8**, 939–948.

[13] Zou J, Glinsky VV, Landon LA, Matthews L, and Deutscher SL (2005). Peptides specific to the galectin-3 carbohydrate recognition domain inhibit metastasis-associated cancer cell adhesion. *Carcinogenesis* **26**, 309–318.

[14] Heimburg-Molinaro J, Almogren A, Morey S, Glinskii OV, Roy R, Wilding GE, Cheng RP, Glinsky VV, and Rittenhouse-Olson K (2009). Development, characterization, and immunotherapeutic use of peptide mimics of the Thomsen-Friedenreich carbohydrate antigen. *Neoplasia* **11**, 780–792.

[15] Glinskii OV, Turk JR, Pienta KJ, Huxley VH, and Glinsky VV (2004). Evidence of porcine and human endothelium activation by cancer-associated carbohydrates expressed on glycoproteins and tumor cells. *J Physiol* **554**(pt 1), 89–99.

[16] Glinskii OV, Huxley VH, Glinsky GV, Pienta KJ, Raz A, and Glinsky VV (2005). Mechanical entrapment is insufficient and intercellular adhesion is essential for metastatic cell arrest in distant organs. *Neoplasia* **7**, 522–527.

[17] Glinsky VV, Glinsky GV, Glinskii OV, Huxley VH, Turk JR, Mossine VV, Deutscher SL, Pienta KJ, and Quinn TP (2003). Intravascular metastatic cancer cell homotypic aggregation at the sites of primary attachment to the endothelium. *Cancer Res* **63**, 3805–3811.

[18] Johnson KD, Glinskii OV, Mossine VV, Turk JR, Mawhinney TP, Anthony DC, Henry CJ, Huxley VH, Glinsky GV, Pienta KJ, et al. (2007). Galectin-3 as a potential therapeutic target in tumors arising from malignant endothelium. *Neoplasia* **9**, 662–670.

[19] Glinsky VV, Kiriakova G, Glinskii OV, Mossine VV, Mawhinney TP, Turk JR, Glinskii AB, Huxley VH, Price JE, and Glinsky GV (2009). Synthetic galectin-3 inhibitor increases metastatic cancer cell sensitivity to taxol-induced apoptosis *in vitro* and *in vivo*. *Neoplasia* **11**, 901–909.

[20] Nangia-Makker P, Hogan V, Honjo Y, Baccarini S, Tait L, Bresalier R, and Raz A (2002). Inhibition of human cancer cell growth and metastasis in nude mice by oral intake of modified citrus pectin. *J Natl Cancer Inst* **94**, 1854–1862.

[21] Glinsky GV, Mossine VV, Price JE, Bielenberg D, Glinsky VV, Ananthaswamy HN, and Feather MS (1996). Inhibition of colony formation in agarose of metastatic human breast carcinoma and melanoma cells by synthetic glycoamine analogs. *Clin Exp Metastasis* **14**, 253–267.

[22] Glinsky GV, Price JE, Glinsky VV, Mossine VV, Kiriakova G, and Metcalf JB (1996). Inhibition of human breast cancer metastasis in nude mice by synthetic glycoamines. *Cancer Res* **56**, 5319–5324.

[23] Platt D and Raz A (1992). Modulation of the lung colonization of B16-F1 melanoma cells by citrus pectin. *J Natl Cancer Inst* **84**, 438–442.

[24] Inohara H and Raz A (1994). Effects of natural complex carbohydrate (citrus pectin) on murine melanoma cell properties related to galectin-3 functions. *Glycoconj J* **11**, 527–532.

[25] Pienta KJ, Naik H, Akhtar A, Yamazaki K, Replogle TS, Lehr J, Donat TL, Tait L, Hogan V, and Raz A (1995). Inhibition of spontaneous metastasis in a rat prostate cancer model by oral administration of modified citrus pectin. *J Natl Cancer Inst* **87**, 348–353.

[26] Inohara H and Raz A (1995). Functional evidence that cell surface galectin-3 mediates homotypic cell adhesion. *Cancer Res* **55**, 3267–3271.

[27] Kuwabara I and Liu FT (1996). Galectin-3 promotes adhesion of human neutrophils to laminin. *J Immunol* **156**, 3939–3944.

[28] Inohara H, Akahani S, Koths K, and Raz A (1996). Interactions between galectin-3 and Mac-2–binding protein mediate cell-cell adhesion. *Cancer Res* **56**, 4530–4534.

[29] Yu LG (2007). The oncofetal Thomsen-Friedenreich carbohydrate antigen in cancer progression. *Glycoconj J* **24**, 411–420.

[30] Nangia-Makker P, Honjo Y, Sarvis R, Akahani S, Hogan V, Pienta KJ, and Raz A (2000). Galectin-3 induces endothelial cell morphogenesis and angiogenesis. *Am J Pathol* **156**, 899–909.

[31] Fukushi J, Makagiansar IT, and Stallcup WB (2004). NG2 proteoglycan promotes endothelial cell motility and angiogenesis via engagement of galectin-3 and $\alpha_3\beta_1$ integrin. *Mol Biol Cell* **15**, 3580–3590.

[32] Nakahara S, Oka N, and Raz A (2005). On the role of galectin-3 in cancer apoptosis. *Apoptosis* **10**, 267–275.

[33] Giguère D, Bonin MA, Cloutier P, Patnam R, St-Pierre C, Sato S, and Roy R (2008). Synthesis of stable and selective inhibitors of human galectins-1 and -3. *Bioorg Med Chem* **16**, 7811–7823.

[34] Rabinovich GA, Cumashi A, Bianco GA, Ciavardelli D, Iurisci I, D'Egidio M, Piccolo E, Tinari N, Nifantiev N, and Iacobelli S (2006). Synthetic lactulose amines: novel class of anticancer agents that induce tumor-cell apoptosis and inhibit galectin-mediated homotypic cell aggregation and endothelial cell morphogenesis. *Glycobiology* **16**, 210–220.

[35] Tejler J, Skogman F, Leffler H, and Nilsson UJ (2007). Synthesis of galactose-mimicking 1*H*-(1,2,3-triazol-1-yl)-mannosides as selective galectin-3 and 9*N* inhibitors. *Carbohydr Res* **342**, 1869–1875.

[36] Fort S, Kim HS, and Hindsgaul O (2006). Screening for galectin-3 inhibitors from synthetic lacto-*N*-biose libraries using microscale affinity chromatography coupled to mass spectrometry. *J Org Chem* **71**, 7146–7154.

[37] Tejler J, Leffler H, and Nilsson UJ (2005). Synthesis of *O*-galactosyl aldoximes as potent LacNAc-mimetic galectin-3 inhibitors. *Bioorg Med Chem Lett* **15**, 2343–2345.

[38] Cumpstey I, Sundin A, Leffler H, and Nilsson UJ (2005). C2-symmetrical thiodigalactoside bis-benzamido derivatives as high-affinity inhibitors of galectin-3: efficient lectin inhibition through double arginine-arene interactions. *Angew Chem Int Ed Engl* **44**, 5110–5112.

[39] Salameh BA, Cumpstey I, Sundin A, Leffler H, and Nilsson UJ (2010). 1*H*-1,2,3-triazol-1-yl thiodigalactoside derivatives as high affinity galectin-3 inhibitors. *Bioorg Med Chem* **18**, 5367–5378.

[40] Kalikin LM, Schneider A, Thakur MA, Fridman Y, Griffin AB, Dunn RL, Rosol TJ, Shah RB, Rehemtulla A, McCauley LK, et al. (2003). *In vivo* visualization of metastatic prostate cancer and quantitation of disease progression in immunocompromised mice. *Cancer Biol Ther* **2**, 17–21.

[41] Loberg RD, Day LL, Dunn R, Kalikin LM, and Pienta KJ (2006). Inhibition of decay-accelerating factor (CD55) attenuates prostate cancer growth and survival *in vivo*. *Neoplasia* **8**, 69–78.

[42] Mossine VV, Glinsky VV, and Mawhinney TP (2008). Food-related carbohydrate ligands for galectins. In *Galectins*. AA Klyosov, ZJ Witczak, and D Platt (Eds). Wiley, London, UK. pp. 235–270.

[43] Fukumori T, Kanayama HO, and Raz A (2007). The role of galectin-3 in cancer drug resistance. *Drug Resist Updat* **10**, 101–108.

[44] Nangia-Makker P, Nakahara S, Hogan V, and Raz A (2007). Galectin-3 in apoptosis, a novel therapeutic target. *J Bioenerg Biomembr* **39**, 79–84.

[45] Chauhan D, Li G, Podar K, Hideshima T, Neri P, He D, Mitsiades N, Richardson P, Chang Y, Schindler J, et al. (2005). A novel carbohydrate-based therapeutic GCS-100 overcomes bortezomib resistance and enhances dexamethasone-induced apoptosis in multiple myeloma cells. *Cancer Res* **65**, 8350–8358.

[46] Wang Y, Nangia-Makker P, Balan V, Hogan V, and Raz A (2010). Calpain activation through galectin-3 inhibition sensitizes prostate cancer cells to cisplatin treatment. *Cell Death Dis* **1**, e101.

[47] Al-Mehdi AB, Tozawa K, Fisher AB, Shientag L, Lee A, and Muschel RJ (2000). Intravascular origin of metastasis from the proliferation of endothelium-attached tumor cells: a new model for metastasis. *Nat Med* **6**, 100–102.